Vortex-loop scaling in the three-dimensional XY ferromagnet

Subodh R. Shenoy
*Institute für Theorie der Kondensierten Materie, Universität Karlsruhe, Federal Republic of Germany and School of Physics, University of Hyderabad, Hyderabad 500134, Andhra Pradesh, India**
(Received 27 February 1989)

A three-dimensional (3D) generalization of the two-dimensional Kosterlitz real-space scaling procedure yields scaling equations for the 3D XY vortex-loop fugacity y_l and loop coupling K_l. These agree with the equations obtained by Williams from helium phenomenology. A dominant diverging loop diameter $a \equiv e^l = \xi_- \approx |\epsilon|^{-\nu}$ [$\epsilon \equiv (T - T_c)/T_c$] controls the exponents for the helicity modulus $\rho_s \approx |\epsilon|^{\nu}$, spin-spin correlation length $\propto \xi_-$, specific heat $\alpha = 2 - 3\nu$, and magnetic field response $\gamma = 2\nu$, $\Delta = \frac{5}{2}\nu$, $\delta = 5$. ν is found by linearizing about a fixed point. For a loop core size a_c small compared to the diverging diameter, $a_c/\xi_- \to 0$, a "Gaussian" value $\nu = \frac{1}{2}$ results. An ansatz $a_c(l) \propto a$ is made to represent the onset of screening from crinkled loops: $a_c(l)/a \simeq (K_l)^{\theta}$ with θ the 3D self-avoiding walk exponent ≈ 0.6. This divergent-core ansatz [$a_c(l-)/\xi_- = 0.57$] yields the exponents $\nu = 0.67$, $\gamma = 1.34$, $\alpha = -0.015$. Monte Carlo results of Kohring *et al.* on vorticity suppression are discussed.

I. INTRODUCTION

Topological excitations (vortex points) are known to drive the phase transition in two-dimensional (2D) planar XY ferromagnets[1] and Josephson junction arrays.[2] Real-space scaling methods have been developed[3] for these interacting vortex points.

Recent work indicates that topological excitations could play a role in a variety of other transitions. Monte Carlo simulations of the three-dimensional (3D) XY model show[4] that a suppression of vorticity suppresses the transition out of the ordered phase. This is consistent with Feynman's conjecture[5] of a vortex-loop mechanism for the equivalent 3D superfluid transition. Similar Monte Carlo (MC) work on the suppression of topological excitations in 4D U(1) lattice gauge theories[6] (monopoles) and in 3D O(3) Heisenberg ferromagnets[7] (spin hedgehogs), also shows a supression of the transition.

Topological excitations have also been conjectured to play a role[8] in the 3D solid melting transition, and in liquid-crystal transitions. Vortex loops have been invoked in 3D lattice superconductor models,[9] and porous-media helium models.[9] They may also play a role in (2+1)D capacitive Josephson junction arrays,[10] or the universal resistive transition of granular superconductors.[11] In the context of high-T_c superconductors, resonating-valence-bond models have been mapped onto U(1) lattice gauge theories.[12] Vortex loops and (field-induced) vortex-line wanderings have also been considered.[13]

The extension of 2D XY vortex-point scaling methods[3] to 3D XY vortex loops is thus possibly both of intrinsic and general interest. In this work we attempt such an extension, following earlier work.[14,15]

Nelson and Fisher[14] have used a $D-2$ expansion on the XY model to obtain generalized Kosterlitz scaling equations, with a correlation length exponent $\nu = 1/2(D-2)^{1/2} + O[(D-2)^{1/2}]$. Using 3D helium II phenomenology, Williams[15] has obtained similar equations, but with logarithmic corrections that depend on the ratio of ring diameter a to a finite core size a_c, with $a_c/a \to 0$ as $a \equiv e^l \to \infty$. He finds numerically that $\nu = 0.526$ (between the Nelson-Fisher[14] $\nu = \frac{1}{2}$ and accepted values of $\nu \approx 0.67$) and finds a critical coupling $K_{0c}^{(W)} = 0.174$, $K_{0c} = 0.348$ in our notation.

In this paper, we use standard dual transformations, following Savit,[16] and Banks *et al.*[17] to map the 3D XY partition function with spin-spin coupling K_0 onto that for interacting integer-valued vortex loops. This is just a convenient reexpression of the original variables,[18] each loop representing a toroid of spins.[19] The possibility of a vortex loop description of 3D XY critical behavior was raised by, e.g., Savit[16] and Halperin.[18] A generalized Kosterlitz[3] procedure is used to sequentially integrate out tumbling loops of diameter a, $a + da$ in a low-fugacity expansion. Scaling equations for the loop fugacities y_l and loop coupling K_l follow, and are in agreement with those of Williams.[15] A free-energy scaling equation is also obtained. Scaling effects in a quasiuniform magnetic field are also considered. Although the derivation is for circular loops, the equations may be more general.

From linearizing about a fixed point $dy_l/dl = 0 = dK_l/dl$ at some $l = l_- \to \infty$, one finds a diverging diameter for the largest loop $a = e^{l_-} = \xi_- \propto |\epsilon|^{-\nu}$ as $\epsilon \equiv (T - T_c)/T_c \to 0$. The exponent ν controls the specific heat and magnetic exponents, $\alpha = 2 - 3\nu$, $\gamma = 2\nu$, $\Delta = 5\nu/2$, $\beta = \nu/2$, while $\delta = 5$. The exponent relations hold.

The spin-spin correlation function is dual-transformed to a loop partition function with imaginary test charges, yielding a decay $\sim e^{-R/\xi'}$ with $\xi' \propto \xi_-$: the loop size determines the correlation length. The helicity modulus (or spin-wave stiffness or superfluid density) is similarly determined, $\rho_s \sim \xi_-^{-1} \sim |\epsilon|^{\nu}$.

A short-distance cutoff for the loop self-energy or "core size" a_c enters the scaling equations as a parameter. For a core size $a_c(l)$ relatively finite at transition,

$a_c(l)/a \to 0$ as $a \to \infty$, we find $\nu = \frac{1}{2}$, consistent with the leading[14] $(D-2)$.

The self-energy per loop segment (per coupling constant), $E_l/K_l \equiv \bar{E}_l \sim \ln(a/a_c)$ appears as a useful parameter. The critical exponent ν can be written as a series $\nu = \frac{1}{2}[1+0(1/\bar{E}_{l_-})]$, with $\bar{E}_{l_-} \to \infty$ for finite cores as $T \to T_c^-$, but a constant for a divergent core.

We consider a divergent-core ansatz, $a_c(l) \propto a$ as $l \sim l_- \to \infty$, intended to represent the crinkling and screening of large loops, not included in the simple scaling analysis. The scale dependence enters through the coupling constant, $a_c(l)/a \approx K_l^{\theta}$, where $\theta = 0.6$ is the 3D self-avoiding walk exponent. One finds then $\nu = 0.67, \gamma = 1.34$, and $\alpha = -0.015$ close to[20] theoretical 3D XY and experimental helium values. With this ansatz the fugacity at transition remains small, $y_{l_-} \to 0.062$, the coupling is parameter independent, $K_{l_-} \to 0.3875$, and the loops at transition are (just barely) well defined, $a_c(l_-)/\xi_- = 0.57$, <1. The 3D XY transition temperature coupling is estimated as $K_0(T_c) \simeq 0.453$, fortuitously close to series solution values[4] of 0.454 ± 0.001.

The paper is divided as follows. In Sec. II we outline the standard dual transform of the 3D XY spin model to a 3D vortex-loop model on a dual lattice. A separation of link variables $J_\mu^{(L)}(r) = \pm 1$ on different loops L yields loop-loop interactions $(L \neq L')$ and self-energy $(L = L')$ or fugacity factors. The scaling equations for the fugacity y_l and coupling K_l are obtained. Section III follows conventional critical-point procedure by linearizing the scaling equations around a fixed point and determining the loop size (or correlation) exponent ν from the eigenvalues of the stability matrix. The Appendix considers the scaling of the dual-transformed correlation function and helicity modulus, and the $\langle J_\mu^{(L)}(R) J_\mu^{(L)}(0) \rangle$ loop-segment correlation. In Sec. IV the scaling equations are generalized to include an external gauge field, chosen to orient the spins quasiuniformly. The free energy appears in scaled form, yielding exponents γ, Δ, and δ. For nonzero fields h, loops are suppressed beyond a size $a_h \sim h^{-2/5}$. Section V makes a physically motivated ansatz for the core-size to loop-diameter ratio $a_c(l)/a$ for large $l \sim l_- \to \infty$ loops. Exponent values follow. Analogies to 2D XY behavior are noted. The results are discussed in Sec. VI, in the context of other systems.

II. THE SCALING EQUATIONS

The 3D XY ferromagnet partition function for N planar spins $-\pi < \theta_i < \pi$ on a cubic lattice is

$$Z = \prod_{i=1}^{N} \int_{-\pi}^{\pi} \frac{d\theta_i}{2\pi} \exp\left[+K_0 \sum_{\mu,i} \cos(\Delta_\mu \theta_i) \right], \tag{2.1}$$

where Δ_μ is a discrete derivative, and $\mu = 1,2,3$ a directional label in the positive axis directions, for each original lattice site i. This also corresponds to a 3D Josephson junction array. A standard dual transform[16] maps (2.1) onto a vortex-loop[10(b),16(a),17] partition function.

A Fourier expansion yields, following Savit,[16]

$$\exp\left[K_0 \sum_{\mu,i} \cos(\Delta_\mu \theta_i) \right] = \sum_{\{n_{\mu,i}\}} \exp[V(\{n_{\mu,i}\})] \exp\left[2\pi i \sum_{\mu,i} n_{\mu,i} \Delta_\mu \theta_i \right], \tag{2.2}$$

where the Fourier label $n_{\mu,i} = 0, \pm 1, \pm 2, \ldots$ is on the bonds of the original lattice. Integrating over θ_i gives

$$Z = \sum_{\{n_{\mu,i}\}} e^{V(\{n_{\mu,i}\})} \prod_i \delta\left[\sum_\mu \Delta_\mu n_{\mu,i} \right], 0 \tag{2.3}$$

with a Kronecker δ loop constraint on $n_{\mu,i}$. It is more convenient to consider low-temperature variables, replacing $n_{\mu,i}$ by the curl of dual-lattice bonds (see Fig. 1) to satisfy the constraint as an identity.[16] With a Poisson summation formula

$$Z = \sum_{\{J_\mu(r)\}} \int_{-\infty}^{\infty} d\phi_\mu(r) \exp[V(\{\epsilon \Delta \phi\})] \times \exp\left[2\pi i \sum_{r,\mu} J_\mu(r) \phi_\mu(r) \right], \tag{2.4}$$

where $(\epsilon \Delta \phi)_\mu(r) \equiv \sum_{\nu,\lambda} \epsilon_{\mu\nu\lambda} \Delta_\nu \phi_\lambda(r)$ is a discrete dual-lattice curl. Here $\phi_\mu(r)$ is a dual-lattice continuum field and $J_\mu(r)$ are the integer-valued vortex-loop variables

$$\sum_{\mu=1}^{3} \Delta_\mu J_\mu(r) = 0, \quad \forall r \tag{2.5}$$

and we will neglect improbable J_μ that begin and end on the boundaries. Throughout the paper, variables labeled with a subscript, like θ_l and $n_{\mu,i}$, are on the original lattice; those with an argument like $J_\mu(r)$ are on the dual lattice.

The transformation so far is exact, but in a low-temperature K_0^{-1} expansion the Fourier coefficient is Gaussian expanded, $e^{V(x)} \approx e^{-x^2/2K_0}$. Doing the $\phi_\mu(r)$

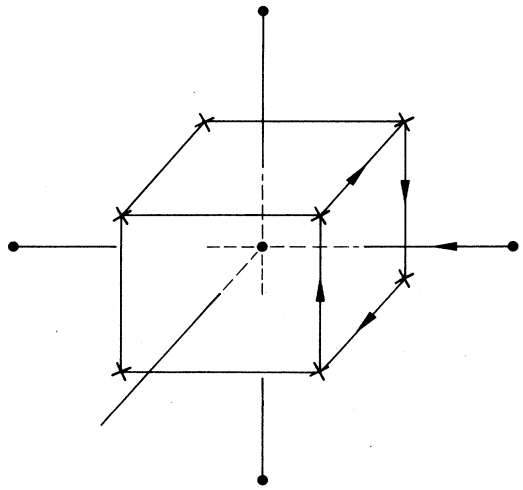

FIG. 1. Original-lattice points (dots), dual-lattice points (crosses), and some bond variables (arrows). An original-lattice bond can be written in terms of dual-lattice bonds, on edges of the dual plaquette it pierces.

integration, one obtains[10(b),11,17]

$$Z=\sum_{\substack{\{J_\mu(r)\}\\ \text{config}}}{}'\exp\left[-\pi\frac{K_0}{2}\sum_{\mu=1}^{3}\sum_{r\neq r'}J_\mu(r)U(r-r')J_\mu(r')\right], \tag{2.6}$$

where the prime on the configuration sum denotes the (2.5) loop constraint and $U(r-r')$ is the 3D lattice Green's function

$$\sum_{\mu=1}^{3}\Delta_\mu^2 U(r-r')=-4\pi\delta_{r,r'}, \tag{2.7}$$

and asymptotically,

$$U(r-r')\simeq\frac{a_0}{|r-r'|}. \tag{2.8}$$

Here a_0 is bare scale, related to the lattice constant that is set equal to unity. Equation (2.6) is then a Biot-Savart law for "topological currents" $J_\mu(r)$ with a sign flip coming from the pure imaginary coupling of (2.4) to the "topological vector potential" $\phi_\mu(r)$.

Labeling the different loops by L, the vortex variables can be divided into those that belong to a given loop, i.e., $\{J_\mu(r)\}\rightarrow\{\{J_\mu^{(L)}(r=r^{(L)})\}\}$. Here $\mathbf{r}^{(L)}=\mathbf{R}^{(L)}+\rho^{(L)}$ where $\mathbf{R}^{(L)}$ is an origin attached to a given loop L, from which the segment position $\rho^{(L)}$ is measured. Restricting ourselves to $J_\mu(r)=0,\pm1$ for low-fugacity reasons, branched loops are forbidden. For circular loops, $\mathbf{R}^{(L)}$ is conveniently chosen as the loop center. Then the J-J interaction in (2.6) splits into a self-energy $J^{(L)}-J^{(L)}$ part and a loop-loop $J^{(L)}-J^{(L')}$ interaction part, $L\neq L'$. Equation (2.5) is satisfied for each loop,

$$\sum_{\mu=1}^{3}\Delta_\mu J_\mu^{(L)}(r)=0,\quad\forall L,r. \tag{2.9}$$

For large, circular loops of *diameter* a_L, the self-energies are, using classical vortex continuum results,[21]

$$\frac{\pi K_0}{2}\sum_{r\neq r'}\sum_{L}J_\mu^{(L)}(r)U(r-r')J_\mu^{(L)}(r')$$

$$=\pi^2K_0\sum_L a_L\left[\ln\frac{a_L}{a_c'}+c_0\right]. \tag{2.10}$$

Here the first factor on the right $\sim a_L$, comes from the loop perimeter $p_L=\pi a_L$, each link a_0 contributing once. The logarithmic factor $\sim\ln(a_L/a_c')$ comes from the angular integration of segments interacting through the $|r-r'|^{-1}$ potential, with a_L and a_c' the maximum and minimum approaches. Here a_c' is a short-distance cutoff, $\propto a_0$ in the bare case. c_0 is related to a core energy, and (2.10) matches[21] the energy per unit length of a straight-line vortex. With a solid-vorticity core assumption,[21(a)] i.e., the same vorticity enclosed for all encircling paths, $c_0=0.329$. For a density variation set by the Ginzburg-Pitaeveskii equation for helium vortices,[21(b)], $c_0=0.464$. (Williams[15] has considered the latter value; his coupling is half ours, $K_0^{(W)}=\frac{1}{2}K_0$.) We define $a_c\equiv a_c'e^{-c_0}$, absorbing the loop-geometry-dependent c_0 into an effective core size a_c.

It is convenient to absorb the minimum loop size a_0 into the coupling, $K_0a_0\rightarrow K_0$. Then the partition function is, at a general scale a, with $l\equiv\ln(a/a_0)$,

$$Z=\sum_{\substack{\{J_\mu^{(L)}\}\\ \text{config}}}{}'\exp\left[-\frac{\pi K_l}{2}\sum_{L\neq L'}\sum_{\substack{\mu,\\ r,r'}}J_\mu^{(L)}(r)U(r-r')J_\mu^{(L')}(r')\right]$$

$$\times y_l^{\sum_L(a_L/a)}\left\{\exp\left[-\pi^2K_l\sum_L\frac{a_L}{a}\ln\frac{a_L}{a}\right]\right\}, \tag{2.11}$$

where now $U(r-r')=1/|r-r'|$, and all distances are scaled in a general minimum loop diameter a. At the initial step of the scaling procedure, $a=a_0, l=0$, and the bare fugacity that carried explicit scale dependence is

$$y_0\equiv e^{-\pi^2K_0\ln(a_0/a_c)}. \tag{2.12}$$

The sum over loop configurations, for N_{tot} circular loops, is written as a configuration integral over loop centers and extents,

$$\sum_{\substack{\{J_\mu^{(L)}(r)\}\\ \text{config}}}{}'\leftrightarrow\sum_{N_{\text{tot}}=0}^{\infty}\sum_{J_\mu^{(L)}=0,\pm1}\frac{1}{N_{\text{tot}}!}\prod_{L=1}^{N_{\text{tot}}}\int\frac{d^3R^{(L)}}{a^3}\int\frac{d^3\rho^{(L)}}{a^3}. \tag{2.13}$$

Here the J sum is over the two possible signs of flow for a given loop and the counting factor takes care of shuffling the loop centers. (The loop segments are directed.)

Although we have considered circular loops for simplicity, the basic structure of the bare self-energy $\sim\pi p_LK_0[\ln(p_L/a_c')+c_L]$ should persist (as can be checked for square geometries, say). Counting factors may differ, but will appear in the latter scaling equations only through a constant A_0 that is found not to affect the critical exponents. Thus the final results may be more general.

The problem (2.11) is the statistical mechanics of current loops interacting through a (sign-flipped) Biot-Savart law, and with various self-inductances and mutual inductances depending on loop size and separation. The loop current $|J_\mu^{(L)}|=1$ is fixed, however. The partition function may be evaluated within a Kosterlitz-Thouless approximation, following the 2D XY prototype calculation closely.

The Kosterlitz-Thouless approximation involves three steps.[1,3] (1) Identification of the simplest, neutral low-temperature configurations of the topological excitations, at a scale a. (2) Integration of the interaction of only such configurations between scales a, $a+da$, with the others that are treated as "far off." This is based on low-fugacity considerations, $y_0<1$. (3) Rescaling of all explicit scale dependences in configuration integrations, interactions, couplings, or self-energies. Absorption of all changes of order $dl\equiv da/a$ into renormalized couplings and fugacities K_l, y_l, recovering the old partition function form.

The 2D procedure[3] is outlined, so we can compare with the 3D case, later. The 2D Coulomb gas partition function is

$$Z=\sum_{\substack{\{m\}\\ \text{config}}}{}'\exp\left[\pi K_l\sum_{r\neq r'}m(r)U(r-r')m(r')\right]\times y_l^{\sum(m^2/2)(r)}, \tag{2.14}$$

where $U(r-r')=\ln(|r-r'|/a)$, $\sum_r m(r)=0$, $m(r)=0,\pm1$, and y_l is the fugacity for a neutral vortex $\pm$*pair* of separation a. The bare fugacity is $y_0=e^{-\pi^2K_0}$. Following step (2) above, the partition function is, symbolically, $Z=Z|_>(1+\delta Z/Z|_>)$ where $Z|_>$ includes only pairs 1,2 of separation greater than $a+da$, and δZ includes only pairs of $a,a+da$ interacting with the larger ones. Thus, with $m(r_1)+m(r_2)=0$,

$$\frac{\delta Z}{Z|_>}\simeq\sum_{m(r_1)=\pm1}y_l\int\frac{d^2R}{a^2}\int\frac{d^2\rho}{a^2}\prod_{\substack{r\\(\neq1,2)}}\{1+2\pi K_l m(r_1)[U(r_1-r)-U(r_2-r)]m(r)\}+\cdots. \tag{2.15}$$

Here $\mathbf{R}$ locates the center of the pair and ρ is the position of one of them, $a/2<\rho<a/2+da/2$. Notice that, since $m(r_1)+m(r_2)=0$, the interaction enters as a difference, $U(r_1-r)-U(r_2-r)\simeq(2\rho)\cdot\nabla_{r_1}U(r_1-r)$. Partial integrations from cross-product terms in (2.14) give $\sim(\rho\cdot\nabla)^2U\sim\frac{1}{2}\rho^2\nabla^2U$ factors, and $\Delta^2U(r)=+2\pi\delta_{r,0}\rightarrow+2\pi a^2\delta(r)$. The ρ integral restrictions give $d^2\rho/a^2=\pi dl$. Reexponentiating, $K_l\rightarrow K_l-4\pi^3y_lK_l^2dl$. Rescaling as in step (3) one has the 2D Kosterlitz scaling equations

$$\frac{dK_l}{dl}=-4\pi^3y_lK_l^2, \tag{2.16a}$$

$$\frac{dy_l}{dl}=(4-2\pi K_l)y_l, \tag{2.16b}$$

$$\frac{d\bar{F}_l}{dl}=\frac{-2\pi y_l}{a^2}, \tag{2.16c}$$

where $\bar{F}_\infty$ is the free energy per area in units of k_BT.

Repeating the procedure in the 3D case, with vortex loops around $L=1$ as the selected neutral configurations

$$\frac{\delta Z}{Z|_>}\simeq\sum_{J^{(1)}=\pm1}y_l\int\frac{d^3R^{(1)}}{a^3}\int\frac{d^3\rho^{(1)}}{a^3}\prod_{\substack{r'\\(L\neq1)}}[1-\pi K_lJ_\mu^{(1)}(r)U(r-r')J_\mu^{(L)}(r')+\cdots], \tag{2.17}$$

where $Z|_>$ contains loops of diameter $a_L>a+da$, for $L\neq1$, and the loops around $L=1$ have $a/2<\rho^{(1)}<a/2+da/2$. The term in curly brackets in (2.11) does not contribute to the prefactor, to $0(dl)$. $J_\mu^{(1)}$ can be written as $J_\mu^{(1)}(\rho^{(1)})$ described with respect to the $L=1$ loop origin $R^{(1)}$.

Since $J_\mu^{(1)}(\rho)=-J_\mu^{(1)}(-\rho)$ for a circular loop, we again have an effective derivative acting on $U(r-r')$ with

$$J_\mu^{(1)}(r)U(r-r')\rightarrow J_\mu^{(1)}(\rho)(2\rho\cdot\nabla)U(\rho+\mathbf{R}-\mathbf{r}').$$

The procedure of partial integrations, angular averages, $(\rho\cdot\nabla)^2U\rightarrow\frac{1}{3}\rho^2\nabla^2U$, and (2.7), carry through with now $d^3\rho/a^3\rightarrow\frac{1}{2}\pi dl$. Reexponentiating, $K_l\rightarrow K_l-A_0y_lK_l^2dl$, with $L=L'$ terms again to be separated in the corrections, generating corrections to the self-energies (2.10).

The square of the charge in the 3D Coulomb case carries dimension energy per length while in the 2D case it has dimensions of energy. Thus step (3) above differs from the 2D case. The coupling K_l occurs both in the self-energy and the interaction. The self-energy term in curly brackets in (2.11) has an explicit length scale $a_L/a=[a_L/(a+da)](1+dl)$ and so we can rescale the coupling K_l in the self-energy by $(1+dl)$ to absorb this. The geometric rescaling of the other K_l in the interaction term, in fact, goes the same way. For general loops the loop diameter a_L and the minimum distance of approach a_0 are the same only for the smallest loops. Large loops can always approach closely, with the bare potential $U=|r-r'|^{-1}\leq a_0^{-1}$. Since we have decided to rescale all distances in loop size a, the potential in these units is larger at the real minimum approach scale, i.e., goes up $(1+dl)$ at each renormalization. Thus the self-energy and interaction couplings are the same K_l, with a purely geometric rescaling $dK_l=K_ldl$, and the 3D scaling equations are

$$\frac{dK_l}{dl}=K_l-A_0y_lK_l^2, \tag{2.18a}$$

$$\frac{dy_l}{dl}=(6-\pi^2 K_l L_l)y_l;\quad L_l\approx\left[\ln\frac{a}{a_c}+1\right], \tag{2.18b}$$

$$\frac{d\bar{F}}{dl}=-\pi\frac{y_l}{a^3}. \tag{2.18c}$$

Here $A_0=4\pi^3/3$ and L_l comes from the long-range interaction contribution (2.10) and is essentially the self-energy per segment (per coupling constant). Comparing (2.18) and (2.16), the main difference is in (2.18a), that leads to a fixed point, rather than a fixed line.

The first two (2.18) equations are those obtained by Williams[15] for circular loops from helium phenomenology and the rescaling procedure of Young[1(c)] and José *et al.*,[16] but based on self-energy terms alone. He obtains a factor $A_0=\pi^5/6$, with the correspondence $K_l\to K_l^{(W)}=\frac{1}{2}K_l$. Nelson and Fisher from $D-2$ expansion[14] also find (2.18a) and (2.18b) but with L_l a constant.

The argument could be repeated for square loops, say, where also $J_\mu(\rho)=-J_\mu(-\rho)$, with equations different only in A_0. For general closed loops, a similar pairing occurs, of oppositely directed segments at points somewhere on the closed perimeter. It is possible therefore that the structure of (2.18) holds in general, for simple geometries at least. Now consider approximate solutions of (2.18).

Unlike the 2D case, the coupling K_l can carry a "geometric" scale dependence $\sim e^l$ even if we neglect possible weak scale dependence and set $L_l=L_0$, say. For infinite temperatures, $K_l=0$, (2.18b) gives $y_l=y_0e^{6l}$, i.e., vorticity proliferates. For low temperatures, with $A_0K_ly_l\ll 1$, and for large l,

$$K_l\approx K_0e^l, \tag{2.19a}$$

$$y_l\approx y_0e^{-a/\xi_0};\quad \xi_0=(\pi^2K_0L_0)^{-1}. \tag{2.19b}$$

Thus large loops are suppressed at low temperatures, to a length $\xi_0\propto T$ that moves up with temperature. One seeks, near T_c, the instability of such a low temperature or ordered form: K_l that scales "geometrically" $\sim e^{+l}$ and y_l that falls off exponentially in a, but now controlled by a diverging length scale $\xi_-\to\infty$ as $T\to T_c^-$.

Existing scaling treatments[22] of order-parameter functionals involve linearizing about a fixed point for $l\to\infty$ and finding eigenvalues of a stability matrix. The partition function is scaled up to some diverging correlation length ξ, including the critical region of wave numbers $k\xi>1$, and capturing the critical singularities. For "disorder parameter" scaling, the size of the topological excitations provides a geometric scale. The "fixed" point is at a particular scale $(dY_l/dl)|_{l_-}=0=(dK_l/dl)|_{l_-}$, with $l_-\to\infty$, probing the stability of large loops.

III. LINEARIZED SOLUTIONS

The trivial high- (low-) temperature fixed point is $K_l^*=0$, $y_l^*=y_0e^{6l}$ ($K_l^*=K_0e^l$, $y_l^*=0$). The nontrivial fixed point is

$$K_{l_-}^*=\frac{6/\pi^2}{L_{l_-}};\quad y_{l_-}^*=\frac{1}{A_0K_{l_-}^*} \tag{3.1}$$

with $dy_l/dl|_{l_-}=0=dK_l^*/dl|_{l_-}$ defining a preferred loop scale l_- that is later taken to go to infinity. Defining linearization variables by

$$K_l\equiv K_l^*(1+\tilde{K}_l),\quad y_l\equiv y_l^*(1+\tilde{y}_l) \tag{3.2}$$

one obtains, for $l_-\to\infty$, a fixed-point stability matrix for large rings

$$\frac{d}{dl}\begin{bmatrix}\tilde{y}_l\\ \tilde{K}_l\end{bmatrix}=\begin{bmatrix}0 & -6\\ -1 & -1\end{bmatrix}\begin{bmatrix}\tilde{y}_l\\ \tilde{K}_l\end{bmatrix}, \tag{3.3}$$

where the geometry-dependent A_0 does not appear. Note that $\tilde{y}_l$, $\tilde{K}_l$ are scaled deviations around l_-, and not simple increments. K_l^*, y_l^* are at most logarithmically varying in loop size, with zero slope at l_-.

Expanding in eigenstates $A_\pm(l)\equiv A_\pm e^{\lambda_\pm l}$, as $\tilde{y}_l=-\sum_\pm 6A_\pm(l)/\lambda_\pm$, $\tilde{K}_l=\sum_\pm A_\pm(l)$, the eigenvalues are $\lambda_\pm=\frac{1}{2}(-1\pm\sqrt{1+24})$ or $\lambda_+=2$, $\lambda_-=-3$. This defines[22] fast-relevant and slow-irrelevant axes in the y_l-K_l plane, of scale dependences that become increasingly or decreasingly important at larger distances. We assume following the existing procedure that the relevant scaling field A_+ is the temperature axis: $A_+\approx A|\epsilon|$, where $|\epsilon|\equiv|(T-T_c)/T_c|$, and A is a constant.

Then the free-energy scaling of (2.18c) implies carrying out the partition function rescaling up to some l:

$$\begin{aligned}Z(K_0,y_0)&=e^{-(\bar{F}_l-\bar{F}_0)L^3}Z(K_l,y_l)\\&=e^{-(\bar{F}_l-\bar{F}_0)L^3}Z(A|\epsilon|e^{\lambda_+ l},A_-e^{\lambda_- l}).\end{aligned} \tag{3.4}$$

We stop scaling[22] at some divergent loop size $l=l_-=\ln(\xi_-/a_0)$, where $l_-\to\infty$ as $|\epsilon|\to 0$. This captures the "critical region" of fluctuation wave numbers $k\xi_->1$. Then, setting $l=l_-\to\infty$, $Z(A|\epsilon|e^{\lambda_+ l_-},0)$ is well defined only if

$$\xi_-=a_0|\epsilon|^{-\nu} \tag{3.5a}$$

and

$$\nu=\lambda_+^{-1}. \tag{3.5b}$$

From (3.3), $\nu=\frac{1}{2}$ in agreement with the leading $D-2$ expansion.[14]

The diverging loop size ξ_- controls the fugacity falloff. Following Williams[15] and removing the nonthermal or geometric scale dependence of the coupling by defining

$$\rho_l\equiv e^{-l}K_l, \tag{3.6}$$

(2.18a) yields

$$\frac{d\rho_l}{dl}=-A_0y_le^l\rho_l^2. \tag{3.7}$$

A series solution for ρ_l in y_l gives, with (2.18b), ρ_∞ some asymptotic value, and $l\gg l_-$

$$\rho_l\approx\rho_\infty+\frac{A_0}{\pi^2L_{l_-}}\rho_\infty y_l. \tag{3.8}$$

Using (3.8) and (2.18b) the fugacity fall off confirms that

only loops $a \leq \xi_-$ are significant:

$$y_l \approx y_0 e^{-6a/\xi_-} . \tag{3.9}$$

Here, from (3.1) and (3.6) the dominant loop size controls the asymptotic ρ_∞ value; with a blow out of y_l and a vanishing of ρ_∞ at transition

$$\rho_\infty \simeq \rho_{l_-} = K^*_{l_-} e^{-l_-} = \frac{(6/\pi^2)}{L_{l_-}} \frac{a_0}{\xi_-} . \tag{3.10}$$

See Fig. 2.

For later use, we note that near l_-

$$K_l \approx K^*_{l_-} e^{l-l_-} + 0(l) . \tag{3.11}$$

[Note that (3.9) and (3.11) are like the low-temperature forms (2.19).] In Sec. IV one finds the superfluid density or helicity modulus $\rho_s \propto \rho_\infty$, so this also vanishes at the loop-size divergence transition.

The free-energy scaling (2.18c) gives with the asymptotic solution (3.9)

$$\bar{F}_\infty \sim \int_0^\infty \frac{da}{a^4} e^{-6a/\xi_-} \sim \frac{1}{\xi_-^3} \sim |\epsilon|^{3\nu} \tag{3.12}$$

so the specific-heat exponent is of the[22] Josephson form,

$$\alpha = 2 - 3\nu . \tag{3.13}$$

Thus as $T \to T_c^-$, the loop size diverges, the fugacity falloff fails, large loops proliferate, the superfluid density spin-wave stiffness falls to zero, and the free energy is singular.[5]

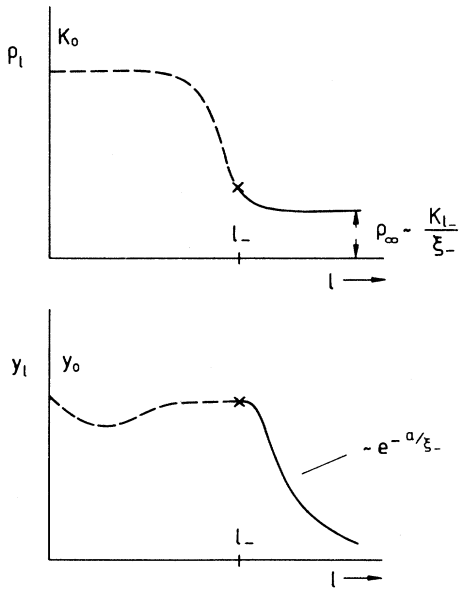

FIG. 2. Schematic plot of the loop coupling $\rho_l \equiv K_l e^{-l}$ geometric scale dependence removed) and the loop fugacity y_l, vs log of the loop diameter $l \equiv \ln(a/a_0)$. Here a_0 is the minimum loop scale, $l_- \equiv \ln(\xi_-/a_0)$ is the log of the dominant diverging loop size $\xi_- \sim (T_c - T)^{-\nu}$ and K_0, K_{l_-} are approximately constants. As temperature $T \to T_c^-$ l_- moves out and asymptotic values of ρ_l (y_l) fall (rise).

The critical temperature can be estimated[22] by setting $|\epsilon| = 0$ for fixed scale $l \neq l_-$ in the linear solution

$$A_+(l) = A|\epsilon| e^{\lambda_+ l} = \tfrac{-1}{6}(\lambda_+^{-1} - \lambda_-^{-1})^{-1}(\tilde{y}_l + 6\tilde{K}_l/\lambda_-) .$$

For $l = 0$, the critical coupling is

$$K_{oc} \approx K^*_{l_-} + \frac{|\lambda_-|}{6}\left[\frac{y_0}{y^*_{l_-}} - 1\right] K^*_{l_-} , \tag{3.14}$$

similar in structure to the 2D result[3] $K_{oc} \approx K^* + 4y_{oc}^{1/2}$. The weak scale dependence in L_{l_-} prevents a sensible result, within linearization. But in Sec. V a finite L_{l_-} ansatz is used to estimate K_{oc}.

In obtaining (3.3) we have dropped terms in $1/L_{l_-} \to 0$ for a fixed a_c. It is useful to go back and retain these terms, but for a general core assumption

$$\frac{a}{a_c(l)} = d_0 \frac{a^\mu}{K_l^\theta} , \tag{3.15}$$

where d_0, μ, and θ are constants, and now $L_l \simeq L_{l_-}(1 - \theta\tilde{K}_l/L_{l_-})$. The matrix of (3.3) is modified [in particular, $6 \to 6(1 - \theta/L_{l_-})$] and one gets

$$\nu \approx \frac{1}{2}\left[1 + \frac{\mu}{5L_{l_-}} + \frac{3}{5}\frac{\theta}{L_{l_-}}\right] + 0\left[\frac{1}{L_l^2}\right] . \tag{3.16}$$

For $\mu > 0$, $L_{l_-} \to \infty$, and ν is unchanged from $\frac{1}{2}$. "Finite" cores $a_c(l)/a \sim a^{-\mu} \to 0$, which do not compete with diverging loop sizes, do not affect the critical exponents, at least within this simple fixed-point linearization. A shift of ν towards its accepted value of 0.67 can only occur if $\mu = 0$ and core sizes diverge like the loop size, so the energy per loop segment $\sim L_{l_-}$ is finite (and if $\theta > 0$). This is considered in Sec. V.

In the Appendix, we consider the scaling of correlation functions by mapping them onto partition functions with imaginary test charges, and then using the results of Sec. II. One finds the spin-spin correlation length ξ' is determined by the loop diameter, ξ_-:

$$\langle \cos(\theta_i - \theta_k) \rangle \propto e^{-R/\xi'}; \quad \xi' = \left[\frac{8\pi K_0^2}{K_{l_-}}\right] \xi_- . \tag{3.17}$$

Long-range order quantities like $\langle \cos\theta_i \rangle$ are not evaluated, but it is likely that the order parameter squared $\langle \cos\theta_i \rangle^2$ goes like the superfluid density ρ_s.

The long-wavelength helicity modulus[17(b),23] or equivalently the superfluid density is determined by the asymptotic value of the coupling in (3.6)

$$\rho_s \propto \rho_\infty \sim |\epsilon|^\nu . \tag{3.18}$$

Thus the superfluid density exponent u is

$$u = \nu$$

and if $\rho_s \sim \langle \cos\theta_i \rangle^2$, and $\langle \cos\theta_i \rangle \sim |\epsilon|^\beta$,

$$\beta = \nu/2 . \tag{3.19}$$

For simple loops, $J_\mu^{(L)}(\rho) = -J_\mu^{(L)}(-\rho)$ on the same loop

L, and the segment-segment correlation

$$\langle J_\mu^{(L)}(r)J_\mu^{(L)}(r')\rangle \propto -\frac{\rho_\infty}{|r-r'|}\ , \tag{3.20}$$

i.e., the contribution from such simple loops vanishes as $T\to T_c^-$.

IV. MAGNETIC FIELD EFFECTS

An external magnetic field couples to a spin pattern $\{\theta_i\}$ through $-\sum_i h_i\cos\theta_i$. Any spin pattern θ_i can in general be regarded as formed from single-valued spin-wavelike deviations, and vortex rotational spin flows. MC work indicates[4] that it is the vortex loops (on the dual lattice) that drive the transition out of the ordered phase. Thus we consider, instead of h_i, a gauge-field $A_{\mu,i}$ that can be more easily dual transformed, that couples to the vortex loops and yet produces a quasiuniform spin orientation. We consider

$$\beta H=-K_0\sum_{\mu,r}\cos(\Delta_\mu\theta_r-A_{\mu,r})\ , \tag{4.1}$$

where $A_{\mu,r}$ is an externally fixed bond variable. For weak fields,

$$\beta H\simeq -K_0\sum_{\mu,r}\cos\Delta_\mu\theta_r-K_0\sum_{\mu,r}A_{\mu,r}\sin\Delta_\mu\theta_r\ . \tag{4.2}$$

Let us take

$$A_{\mu,r}=\tfrac{1}{2}\epsilon_{\mu\nu\lambda}\frac{r_\nu}{a_0}h_\lambda(r);\quad \sum_{\mu=1}^{3}\Delta_\mu A_{\mu,r}=0\ , \tag{4.3}$$

where $\mathbf{r}$ is an original lattice position, and $h(r)$ some slowly varying field. Then the coupling term is $\sim -\mathbf{h}\cdot(\mathbf{r}\times\sin\Delta\theta_r)$. In the 3D Josephson array language, $\sin\Delta_\mu\theta_r$ is a supercurrent and so, with such a coupling, the variable $\mathbf{h}(r)$ (taken in the z direction, say) can couple to circulating supercurrents round an elementary lattice face. A vortex loop is an extended object of such circulations.[16(a),19] To determine the coupling between the field $\mathbf{h}$ and the loops, one repeats the dual transform of (2.2)–(2.4), with now $\Delta_\mu\theta_r-A_{\mu,r}$ in the argument of the exponential in (2.2). Once again, one goes to a dual lattice, and now defines additional dual variables $A_\mu(r)$, by

$$A_\mu(r)=\sum_{\nu,\lambda=1}^{3}\epsilon_{\mu\nu\lambda}\Delta_\nu A_{\lambda,r}\ , \tag{4.4}$$

where $A_\lambda(r)$ is along the edges of the dual-lattice plaquette pieced by the original-lattice bond.[16(a)17] For (4.3), $A_\mu(r)$ is $\propto h_z(r)\delta_{\mu,z}$.

One finds, on the dual lattice, that (2.4) is replaced by

$$Z=\sum_{\substack{\{J\}\\ \text{config}}}\exp\left[-\frac{\pi K_0}{2}\sum_{\substack{\mu,r\\ r'}}[F_\mu(r)+J_\mu(r)]U(r-r')\right.$$
$$\left.\times[F_\mu(r')+J_\mu(r')]\right], \tag{4.5a}$$

where

$$F_\mu(r)=\sum_{\nu,\lambda}\epsilon_{\mu\nu\lambda}\Delta_\nu A_\lambda(r)/2\pi \tag{4.5b}$$

and with (4.3) $2\pi\mathbf{F}(r)=(\partial h_z/\partial y,-\partial h_z/\partial x,0)$. It is convenient to choose F as a solenoidal "current" along the faces of the system parallel to the solenoid axis z. It generates a "field" h_z parallel to the z axis and almost uniform, except at the edges; for large systems.[23,24] For later use we note that at a general lattice scale a, and away from the system edges, from (4.3) and (4.4)

$$A_\lambda(r)\simeq 2\pi ha\hat{\mathbf{z}}\ . \tag{4.6}$$

Since gauge fields involve line integrals between sites, an explicit scale dependence is appropriate.

Using standard electromagnetic results,[25] the "field" $A_\mu(r)$ is found to orient the topological "moments" of the $J_\mu^{(L)}(r)$ loops. The relevant energy contribution from (5.2) is

$$\beta H=\pi K_0\sum_L\sum_{\mu,r,r'}F_\mu(r)\frac{1}{|r-r'|}J_\mu^{(L)}(r')$$
$$\simeq -2\pi K_0\sum_{L,R}\mathbf{A}(R^{(L)})\cdot\mathbf{M}^{(L)}(R^{(L)})\delta_{R,R^{(L)}}\ , \tag{4.7}$$

where the topological "moment" is

$$M_\mu^{(L)}(R)=\tfrac{1}{2}\sum_{\nu,\lambda}\epsilon_{\mu\nu\lambda}\rho_\nu J_\lambda^{(L)}(\rho)=\frac{\pi a_L^2}{4}(\mathrm{sgn}J_\lambda^{(L)})\hat{\mathbf{M}}_\mu\ . \tag{4.8}$$

Here the center of the loop is the origin, and $\hat{\mathbf{M}}_\mu$ is a unit vector perpendicular to the loop area. The energy of the smallest loop then scales as $\sim ha^3K_0$.

The scaling procedure of Sec. II can then be repeated, now including the extra energy of loops tumbling in a (weak) orienting field.[26] The relevant extra contribution to (2.15) is, with (4.7),

$$\frac{\delta Z}{Z|_>}\simeq\sum_{J=\pm1}y_l\int\frac{d^3R}{a^3}\int\frac{d^3\rho}{a^3}(\pi^4K_lh)^2(\hat{\mathbf{M}}\cdot\hat{\mathbf{Z}})^2a^6\delta^{(3)}(R)\ . \tag{4.9}$$

This modifies the constant or free-energy contribution to

$$\frac{d\bar{F}}{dl}=\frac{\pi y_l e^{-B_0h^2a^3K_l^2}}{a^3}\equiv\frac{\pi y_l(h)}{a^3}\ , \tag{4.10}$$

where $B_0\equiv(\pi^8/3)$ and a field-dependent fugacity $y_l(h)$ has been defined.

The scaling of the coupling and self-energies carries through, and (2.18a) is unchanged in structure

$$\frac{dK_l^{-1}}{dl}=-K_l^{-1}+A_0y_l(h) \tag{4.11}$$

with $y_l(h)$ now obeying

$$\frac{dy_l(h)}{dl}\approx(6-\pi^2K_lL_l-5B_0h^2a^3K_l^2)y_l(h)\ . \tag{4.12}$$

This implies that for scales beyond

$$a_h\sim\frac{1}{(B_0K_0^2)^{1/5}}h^{-2/5} \tag{4.13}$$

the usual scaling flows are diverted. The low-

temperature fixed point $y_l^*=0$, $K_l^*=K_0 e^l$ dominates at all T. Fugacities fall off as $e^{-h^2a^5}$: large loops are suppressed by their cost in a field.

Using $y_l(h)$, with the right limiting fugacity forms,

$$\bar{F}_\infty \sim \int_0^\infty \frac{da}{a^4} e^{-6a/\xi_-} e^{-B_0 K_0^2 h^2 a^5} \sim |\epsilon|^{3\nu} f\left[\frac{h}{|\epsilon|^\Delta}\right], \tag{4.14}$$

where the integral defines a function f in scaling form.[22] The exponents are read off as

$$\gamma=2\nu\,, \quad \delta=5\,, \quad \Delta=\frac{5\nu}{2}\,, \tag{4.15}$$

for $\nu=\frac{1}{2}$, $\gamma=1$, and $\Delta=\frac{5}{4}$.

It is easy to check that the scaling relations[22] such as $\alpha+2\beta+\gamma=2$, $\gamma=\beta(\delta-1)$, $\gamma=(2-\eta)\nu$, or $\beta=2-\alpha-\Delta$, $\gamma=-2+\alpha+2\Delta$ are satisfied for general ν, by the forms of (3.13), (3.19), and (4.15). The divergent loop size $\xi_-\sim|\epsilon|^{-\nu}$ or correlation length, controls the other exponents.

V. ANSATZ FOR SCALE-DEPENDENT CORE SIZE

There are two length scales associated with 3D vortex loops, namely, the overall size or diameter a_L, and the (effective) core size a_c. The self-energy of a loop is $\sim a_L \ln(a_L/a_c)$, with the unscreened $1/R$ potential producing an energy per unit length that depends on size. The transition caused by the size blow up yields Gaussian-like exponents, $\nu=\frac{1}{2}$, so some physical idea is missing. One pictures a second-order transition as involving a blowup of fluctuations of the "wrong" phase, as T_c is approached. Since the high-temperature phase is a "tangled mass of vorticity," with randomly wandering lines, we consider random crinkling of vortex loops,[17] even below T_c, and its effects on the only other length, a_c.

The crinkling of loops will have several effects. The minimum approach distance will depend on the amount of crinkling, that increases with the loop diameter $a\equiv e^l$. Since lengths appear as ratios, the core size acquires a scale dependence $a_c\to a_c(l)$, that absorbs these random-walk excursions around the average circular geometry.

The crinkling should also produce partial vector cancellations of the effects of the $J_\mu(r)$ segments. Moreover the crinkling permits other crinkled and twisted loops to screen more efficiently than the "dipolar" loop screening considered so far. From (2.10) the size dependence $\sim\ln a$ of the energy per unit length comes from the large-distance $\sim a$ segments of the loop seeing the $1/R$ potential. Thus if we assume only nearby segments $\sim\lambda$ interact via $1/R$, we make the replacement

$$\frac{a_c(l)}{a}\to\frac{a_c(l)}{\lambda}\,, \tag{5.1}$$

where λ is some screening length.

The random-walk extent of these λ segments of loops of size a should scale as a^θ where θ is a 3D *self-avoiding* walk exponent. (Walks that cross can be regarded as involving smaller loops that have just touched the simpler, self-avoiding loop at the crossing point. These are already included in the scaling.) K_l carries a geometric scale, and in fact controls the tendency of attracting segments to bend towards each other. We assume the length dependence enters only through the coupling, $a_c(l)/\lambda\sim a^\theta\sim K_l^\theta$. Thus, finally, ansatz is, from (3.11),

$$\frac{a_c(l)}{a}=K_l^\theta=(K_{l_-}e^{l-l_-})^\theta=K_{l_-}^\theta\left[\frac{a}{\xi_-}\right]^\theta \tag{5.2}$$

for large rings l near $l_-\gg1$. The core size or crinkling region is proportional to the loop diameter, and diverges with it. Note that the ansatz uses the core parameter $a_c\equiv a_c' e^{c_0}$, that absorbs the constant c_0 from the particular geometry seen by the $1/R$ potential. It implies that all large geometries crinkle in the same way.

The helium λ transition is believed to be in the same universality class as the 3D XY model.[5] In helium, the superfluid density drops to zero at the vortex core, which thus contains the high-temperature or normal phase. The size of the normal core blows up[8] at transition. The 3D XY lattice model involves only the phase angle, and does not have such magnitude variation. However, the ansatz of (5.2) could be regarded similarly as the high-temperature (meandering vortex) phase hidden in the effective core, $a_c(l_-)$, that blows up at transition.

The constant K_{l_-} is determined by the fixed-point condition (3.1), from (2.18b) and (6.2):

$$K_{l_-}=\frac{6/\pi^2}{L_{l_-}};\quad L_{l_-}=1-\theta\ln K_{l_-}\,. \tag{5.3}$$

We take $\theta=0.6$, the Flory value $3/(2+D)$ for $D=3$.[27] By substitution one sees that the universal value

$$K_{l_-}=0.3875,\quad L_{l_-}^{-1}=0.6374 \tag{5.4}$$

is a solution. The energy per segment, $E_{l_-}=\pi K_{l_-}L_{l_-}$, is thus a constant, as $T\to T_c^-$. The fixed-point fugacity value $y_{l_-}=(A_0K_{l_-})^{-1}=0.062$ is small, so a fugacity expansion is reasonable right up to T_c. The core- to loop-size ratio is $a_c(l_-)/\xi_-=0.566<1$, so the divergent-core-loop is still (just) defined[8] at transition.

Returning to the procedure[28] of Sec. III and linearizing in $\tilde{K}_l$, $\tilde{y}_l$, and with $L_l\simeq L_{l_-}(1-\theta\tilde{K}_l/L_{l_-})$, the stability matrix only changes by $6\to6(1-\theta/L_{l_-})$. The eigenvalues are $\lambda_\pm=\frac{1}{2}\{-1\pm[24(1-\theta/L_{l_-})]^{1/2}\}$ yielding a correlation exponent

$$\nu=0.6717\,. \tag{5.5}$$

[Compare (3.16) with $\mu=0$.] The other exponents follow,

$$\gamma=1.343,\quad \alpha=-0.015\,. \tag{5.6}$$

These are close to the values[20,22] obtained by diagrammatics, high-temperature, and 4D expansions. For example, high-temperature expansions give[20] $\nu\simeq0.678\pm0.005$,

$\alpha=-0.02\pm0.03$. With (5.2) and (5.3), ν depends only on θ, and a plot of ν versus θ is given in Fig. 3. For $\theta=0$, $\nu=\frac{1}{2}$ while for the value $\theta=0.5745$ one has $\nu=0.6669$, close to $\frac{2}{3}$.

The critical bare coupling can be estimated, using (3.14) and the ansatz, i.e., $6\to6(1-\theta/L_{l_-})$, and the above $|\lambda_-|=2.488$. The effective core size at the initial scale $a=a_0$ is $a_c(0)\equiv a_c' e^{-c_0}$ where [21(a)] $c_0=0.329$ and a_c' is the minimum segment on the loop of radius $\frac{1}{2}a_0$. We take this loop as just enclosing the square face of the unit-length cubic lattice. This defines an appropriate, rotationally averaged, minimum size, set by the lattice. The minimum loop segment a_c' subtended by the unit lattice side is $a_c'=(\pi/2)(\frac{1}{2}a_0)$. Then (2.12) defines $y_{0c}=\exp(-5.63K_{0c})$ and the critical coupling from (3.14) is $K_{0c}\sim0.453$. This is fortuitously close to the series solution estimate,[4] 0.454 ± 0.001.

The ansatz implies that the energy per segment E_{l_-} becomes an intensive quantity as $T\to T_c^-$. This suggests a physical picture for the 3D transition that has some analogies with the 2D case. This follows earlier ideas, on the transition from a high-temperature "spaghetti" phase to a low-temperature "alphabet soup" phase.[16(a),17(a)] (E_l involves essentially the logarithm of the inverse curvature for $1/R$ potentials, so circular segments, with minimum curvature for a given length, could be most sensitive to a breakdown of screening. This supports our earlier concentration on the most tractable, circular, loops.)

The bare energy per $+-$ vortex pair for the 2D case is $E_0=\pi K_0 \ln R$ in the low-temperature phase with the bare form unaltered by dipolar screening. The vortex correlation function is $C(R)=\langle m_R m_0\rangle\sim R^{-\eta-(D-2)}$ with $\eta\neq0$ and $D=2$. In the high-temperature screened phase, $E_{l_+}\sim0(1)$ and $C(R)\sim e^{-R/\xi_+}$. The pair separation a and core size a_c' are the same, $a/a_c'=1$.

The bare energy per segment for oppositely directed $J_\mu(r)$ in the 3D case is $E_0=\pi K_0 \ln R$ in the low-temperature phase. The form is unaltered by loop dipolar screening. The oppositely directed segment-pair correlation is $C(R)=\langle J_\mu^{(L)}(R)J_\mu^{(L)}(0)\rangle\sim\rho_\infty/R$ or $\sim R^{-\eta-(D-2)}$ with $\eta=0$ and $D=3$. As $T\to T_c^-$ crinkling and screening set in at and above transition, where $E_{l_+}\sim0(1)$ and $C(R)\sim e^{-R/\xi_+}$. The segment separation and core size are in a constant ratio, $a_c(l_-)/\xi_-$ fixed, as $T\to T_c^-$.

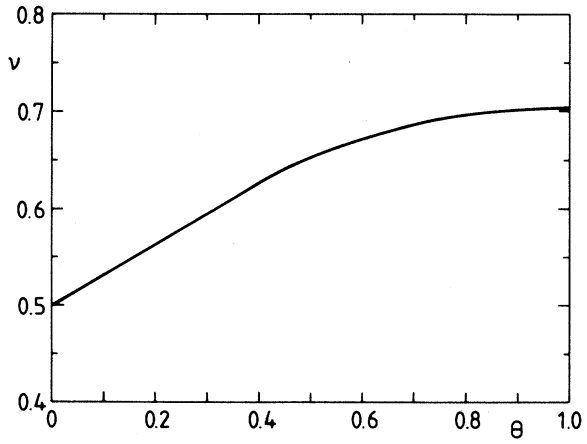

FIG. 3. Spin-spin correlation exponent or loop-size exponent ν vs self-avoiding walk exponent θ, treated as a parameter.

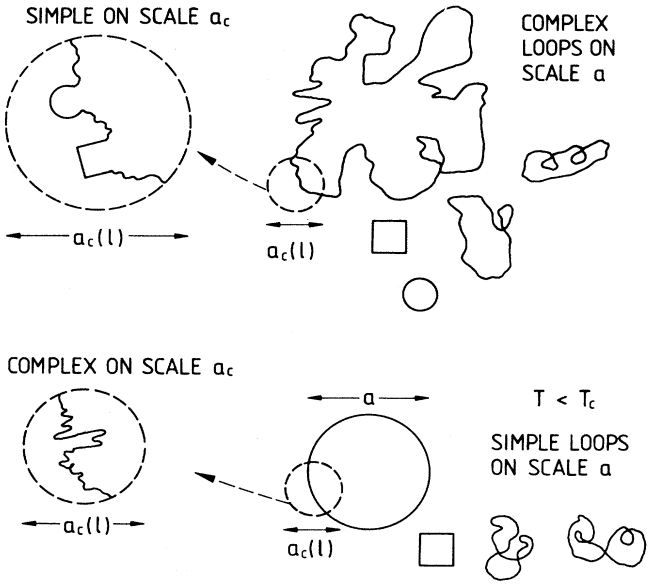

FIG. 4. Conjectured qualitative picture of dominant loop geometries above ($T>T_c$) and below ($T<T_c$) transition. Dashed circles denote magnification of some core scale $a_c(l)$, for loop of diameter $a=e^l$. As $T\to T_c^-$ small simple loops crinkle more violently and over larger scales, as large, complex geometries dominate. As $T\to T_c^+$ complex loops smooth out and smaller simpler geometries pinch off.

Focusing on the role of the energy per segment (per coupling constant) $\bar{E}_l\equiv E_l/K_l$, the following picture of the transition is suggested, as depicted in Fig. 4. For $T>T_c$ the long, meandering, tangled, and possibly knotted or braided loops have no well-defined large-scale geometries and mutually screen each other strongly,[8(a)] so $\bar{E}_l\sim0(1)$. As T decreases, the number of loops decreases and screening decreases. At T_c^+, $\bar{E}_l\sim\ln R$ over a finite fraction of loop regions and the energy cost of being part of a large R loop outweighs the entropy gain.[17(a)] The simpler-geometry segments, that exist on small scales, and that are almost closed, then pinch off. For $T<T_c$ the same[4] total vorticity is distributed into finite-sized loops, now crinkled or bent around a more well-defined geometry. Screening is dipolar and weaker, with $\bar{E}_l\sim\ln R$ favoring smaller loops. In both phases the "wrong" phase, represented by the "wrong" geometry, exists on finite scales $\sim a_c$ that blow up as transition is approached from either side.

VI. DISCUSSION

A scaling approach based on topological excitations has been presented for the 3D XY model, dual

transformed to a 3D vortex-loop model. Within the Kosterlitz-Thouless approximation, the loop scaling equations of Williams are obtained microscopically. The loop diameter $a \equiv e^l$ and core size a_c are two length scales in the problem.

Linearizing the scaling equation around a preferred diverging loop diameter $\xi_- \sim |\epsilon|^{-\nu} \to \infty$ yields the specific-heat exponent $\alpha = 2 - 3\nu$. A simple fixed-point analysis yields $\nu = 0.5$. Corrections in inverse powers of the self-energy per loop segment vanish for finite core size, $a_c/a \to 0$ as $a \to \infty$. (By a numerical procedure Williams finds $\nu = 0.526$ with a finite core; the relation between the two approaches is not clear at present.) The dominant loop size ξ_- controls the falloff of the fugacity and spin-spin correlations and the helicity modulus value. Scaling equations modified to include a particular weak, slowly varying magnetic field, yield magnetic exponents $\gamma = 2\nu$, $\Delta = 5\nu/2$, $\delta = 5$. An ansatz for a scale-dependent core size, $a_c(l)$, to allow for the (divergent) crinkling and screening of loops as $T \to T_c^-$, turns out to yield exponents close to accepted values. A full description of the transition seems to need both loop-size and core-size divergences; neglect of the latter leads to "Gaussian" exponents. The ν exponent value is determined by the space dimensionality and symmetries of the XY Hamiltonian, by the value of π, and by the random-walk exponent appropriate to the topological excitations. The lack of microscopic justification for the core-size scaling ansatz constitutes a weakness of the analysis, however.

Order-parameter-based critical-point methods typically involve short-ranged models, with long-range correlations and scales emerging from renormalization. Critical-point analyses based on topological excitations, or "disorder parameters" have natural long-range interactions and scales, from the start. The two approaches are complementary.[18]

Kohring *et al.*[4] consider an extra weighting term in (2.1) $-\lambda \sum |v|$ where the sum is over original-lattice plaquettes and $|v| = |\sum \Delta_\nu \theta_l / 2\pi|$ round one plaquette is unity for plaquettes pieced by a dual lattice $|J_\nu| = 1$ and zero otherwise. (They also consider the 3D XY antiferromagnet.) The asymptotic $1/R$ vortex interaction should not be affected by this term, that just adds an energy $\sim 2\lambda$ to the vortex energy per unit length. A similar (ferromagnetic) scaling analysis should carry through with a term $\sim 2\lambda \sum J_\mu^2$ and with critical exponents expected to be unchanged. The extra energy cost would inhibit the size blow up, increasing T_c as is found,[4] with a suppression of the transition beyond a critical λ_c that can be estimated. Equation (2.6) should acquire an extra term $\exp[-2\lambda \sum_{\mu,r} J_\mu^2(r)]$. For $K_0 = 0$, the partition function with this term is similar to the (Gaussian) original-lattice partition function of (2.3), where the weight factor is $\exp[-(2K_0)^{-1} \sum_{\mu,i} n_{\mu,i}^2]$. Thus these "self duality"[9(a)] arguments lead to the estimate $\lambda_c \approx (4K_{oc})^{-1} = 0.5518$, close to the MC value.[4] This may be pursued elsewhere.

It would be interesting to see if topological-excitation scaling ideas are useful in other contexts. The anisotropic 3D XY model may be relevant to high-T_c superconductors.[13] Vortex loops have also been considered in lattice superconductor models[9,24] with thermally fluctuating gauge fields. Including radial degrees of freedom, Monte Carlo work shows a first-order phase transition,[9] beyond a tricritical point. One might have to consider the competition between $|J_\mu| = 1$ and $|J_\mu| = 2$ vortex loops,[9(c)] with the lower $|J| = 2$ initial fugacity compensated by the stronger coupling beyond the tricritical point.

Capacitive and dissipative effects in 2D Josephson arrays,[10(a)] motivated by the universal resistive transition of granular superconductors,[11] are of much current interest. One can map the problem at $T = 0$ onto (2+1)D vortex loops[10(b)] with scaling behavior controlled by the capacitances and couplings. Details will be given elsewhere. The low-temperature first-order transition found in MC simulations[10] could be related to (2+1)D (quantum) vortex loops taking over from 2D (classical) vortex lines, as the imaginary time "system size" $\sim T^{-1}$ increases.

Lattice gauge theories like the 4D $U(1)$ model[6] have topological excitations, (monopole strings), but phase diagrams are often evaluated by lengthy MC runs. A scaling analysis could be useful. The 3D Heisenberg model has spin hedgehog excitations that are necessary for the transition.[7] Crystal melting and smectic liquid-crystal transitions could involve appropriate dislocation and/or disclination loops.[8] Topological excitations also play a role in Hubbard-based resonating-valence-bond models of high-T_c superconductors that have been mapped onto lattice gauge models.[12] Friedel[13] has considered the effects of layering in the high-T_c materials on vortex-loop orientation and KT-like effects have been seen in anisotropic bismuth compounds. Nelson[13] has connected the thermal crinkling of field-induced vortex lines to the critical field-temperature phase boundary. Glassy behavior[29] is also of interest.

In summary, following 2D XY methods, a 3D vortex-loop scaling analysis has been developed for the 3D XY model that may be relevant for other models with topological excitations.

ACKNOWLEDGMENTS

It is a pleasure to thank Ulrich Eckern and Albert Schmid for valuable discussions, J. M. Kosterlitz for a stimulating comment, and C. Dasgupta for a copy of his work prior to publication. Partial support of the Alexander von Humboldt Foundation is gratefully acknowledged.

APPENDIX

We evaluate the spin-spin correlation function, the helicity modulus, and the loop-segment correlation, showing that they are all controlled by the diverging loop size. The method, following previous[16(b),23] analysis in the 2D case, is to map the relevant correlations onto a vortex-loop partition function with imaginary test charges at the singled-out bonds. Since the test charges do not affect the scaling equations as system size $N \to \infty$, previous results can be taken over.

Consider the spin-spin correlation function

$$G_{ik}=\langle e^{i(\theta_i-\theta_k)}\rangle-\langle\cos\theta_i\rangle\langle\cos\theta_k\rangle\ . \tag{A1}$$

This can be written as

$$\tilde{G}_{ik}=\left\langle\exp\left[i\sum_{\mu,r}S_{\mu,r}\Delta_\mu\theta_r\right]\right\rangle\ , \tag{A2}$$

where the tilde means we ignore any long-range contributions, and focus only on the fall off produced by fluctuations. Here $S_{\mu,r}=\Delta_\mu\sigma_r$ and

$$\sum_\mu\Delta_\mu S_{\mu,r}=\sum_\mu\Delta_\mu^2\sigma_r=-\delta_{ri}+\delta_{rk} \tag{A3}$$

so a partial integration on (A2) recovers (A1). For a given original-lattice bond variable $S_{\mu,r}$, it is useful to define dual-lattice bond variables $S_\mu(r)$ related by

$$S_{\mu,r}=\sum_{\nu,\lambda}\epsilon_{\mu\nu\lambda}\Delta_\nu S_\mu(r)\ . \tag{A4}$$

These are around the edges of the dual plaquette, pierced by the original-lattice bond, as in Fig. 1.

In the spin-wave (SW) approximation, and on the original lattice

$$\tilde{G}_{ik}\Big|_{\rm SW}\approx\exp\left[\tfrac{-1}{2}\sum_{\mu'r',\mu,r}S_{\mu,r}S_{\mu'r'}\Delta_\mu\Delta_{\mu'}\langle\theta_r\theta_{r'}\rangle\right]$$
$$\approx\exp\left[-\sum\frac{S_{\mu r}^2}{2K_0}\right]\approx e^{(1/4\pi K_0)(1/r_{ik})}\ , \tag{A5}$$

where (A3) has been used, and we present only the asymptotic falloff. Spin waves do not produce exponential decays.

The dual transformation on (A2) carries through as in (2.3), with now a Kronecker δ constraint $\sum_\mu\Delta_\mu(n_{\mu,r}+S_{\mu,r})=0$ satisfied as an identity through going over to dual-lattice variables,

$$n_{\mu r}+S_{\mu,r}\rightarrow\sum_{\nu,\lambda}\epsilon_{\mu\nu\lambda}\Delta_\nu(N_\lambda(r)+S_\lambda(r))\ .$$

Finally one gets, for $K_0^{-1}\ll1$,

$$\tilde{G}_{ik}=\exp\left[-\sum_{\mu,r}S_\mu^2(r)/2K_0\right]$$
$$\times Z[\{J_\mu(r)+i\psi_\mu(r)\}]/Z(\{J\})\ , \tag{A6}$$

where going back to the original lattice and using (A3) the first factor is seen to be the spin-wave contribution of (A5). We have defined pure imaginary test charges, along the dual bonds,

$$i\psi_\mu(r)=\frac{-i}{2\pi K_0}\Delta^2S_\mu(r)\ . \tag{A7}$$

Suppressing vortices, the contribution from

$$Z(i\psi)\equiv\exp[+(\pi K_0/2)\sum\psi_\mu(r)U(r-r')\psi_\mu(r')]$$

is seen to go as $1/r$, like the irrelevant spin-wave contribution.

The scaling procedure then just carries through, with scaling carried out up to $a=r_{ik}\equiv R$ with distances scaled in a, $U(R)\approx1$. Then, $l_R\equiv\ln(R/a_0)$, the asymptotic behavior is dominated by the vortex renormalization:

$$\tilde{G}_{ik}\approx\exp\left[-\frac{\pi K_{l_R}}{2}\sum_{r,r'}\psi_\mu(r)U(r-r')\psi_\mu(r)\right]$$
$$\equiv\exp(-K_{l_R}/4\pi K_0^2) \tag{A8}$$

or, with (3.11)

$$\tilde{G}_{ik}\equiv e^{-r_{ik}/\xi'};\quad\xi'\equiv\left[\frac{4\pi K_{oc}^2}{K_{l_-}}\right]\xi_-\ . \tag{A9}$$

The spin-spin correlation fall off ξ' is thus proportional to (and about ten times larger than) the diameter ξ_- of the dominant tumbling loop, that is only moderately efficient in stirring up the spins. The use of the correlation exponent ν notation in (3.5a) is thus justified.

Since we have not kept track of logarithmic corrections, the exponent η is not evaluated. The exponent relations with (4.15) are consistent with a value $\eta=0$.

Turning to the helicity modulus, similar methods are useful. Regarding the 3D XY model as a 3D Josephson array, the supercurrent induced by an external vector potential is

$$j_{\mu,i}=-\sum_{\nu,k}\Lambda_{\mu,i;\nu,k}A_{\nu,k}\ , \tag{A10}$$

where the response function is the helicity modulus ($A_{\nu k}$ is a "twist") for spin systems[30] or the superfluid density [(A10) is a London equation] for Josephson arrays. Here

$$\Lambda_{\nu,i,\nu,k}=K_0\delta_{\mu\nu}\delta_{ik}\langle\cos\theta_i\rangle-K_0^2\langle\sin\Delta_\mu\theta_i\sin\Delta_\nu\theta_k\rangle\ . \tag{A11}$$

In the spin-wave approximation, it is easy to evaluate (A11), and in the long-wavelength limit, $K_0^{-1}\ll1$, the response is transverse

$$\Lambda(q)\equiv K_0\left[\delta_{\mu\nu}-\frac{q_\mu q_\nu}{q^2}\right]\ . \tag{A12}$$

For a transverse vector potential, only the current-current correlation is relevant and (A11) can be written as

$$\Lambda_{\mu,i;\nu,k}=-K_0^2(1-\delta_{\mu\nu}\delta_{ik})$$
$$\times\sum_{\alpha=\pm1}\tfrac{1}{2}\alpha\left\langle\exp\left[i\sum_{\mu,r}S_{\mu,r}^{(\alpha)}\Delta_\mu\theta_r\right]\right\rangle\ , \tag{A13}$$

where now two bonds are singled out,

$$S_{\lambda,r}^{(\alpha)}\equiv(\delta_{r,k}-\delta_{r+\mu,k})\delta_{\lambda,\mu}+\alpha(\delta_{r,i}-\delta_{r+\nu i})\delta_{\lambda,\nu} \tag{A14}$$

between a widely separated pair of nearest-neighbor sites.

Once again, one can map this onto a partition function with imaginary test charges as in (A6), with $S_\mu^{(\alpha)}(r)$ in (A7). The scaling proceeds as before up to l_R. The differences of nearest-neighbor δ's in (A14) are always on the (original) lattice scale of a_0, i.e., scale as a^{-1}. Thus

$$K_{l_R}\psi^{(\alpha)}U\psi^{(\alpha)}\sim K_{l_R}a/a^2\sim\rho_\infty\ .$$

The final result for the superfluid density $\rho_s = \lim_{q\to 0}\Lambda(q) \sim |\epsilon|^u$ is

$$\rho_s \simeq \rho_\infty \sim |\epsilon|^\nu; \quad u = \nu , \tag{A15}$$

so the superfluid density exponent μ is also determined by the loop divergence exponent ν. In the high-temperature phase, the superfluid density is zero,[8(a)] due to a screened interaction.

The order parameter $\langle \cos\theta_i \rangle$ that involves a test charge rather than test dipoles is not evaluated here, but one expects $\rho_s \sim \langle \cos\theta_i \rangle^2 \sim |\epsilon|^{2\beta}$ or $\beta = \nu/2$.

Finally, we consider the correlation

$$C(R) \equiv \langle J_\mu^{(L_0)}(R) J_\mu^{(L_0)}(0) \rangle$$

between segments on the same loop L_0. Ignoring all loops except this one, the weighting factor

$$\exp[-(\pi K_0/2) J_\mu^{(L_0)}(R) U(R) J_\mu^{(L_0)}(0)]$$

gives $C(R) \simeq -2\pi^2 K_0/R a_0$. This is modified by dipolar loop screening to

$$C(R) \equiv -2\pi^2 \rho_\infty / R \tag{A16}$$

the fraction of simple-geometry loops vanishing as $T \to T_c^-$. Since diametrically opposite segments are directed oppositely (for circular loops) this is analogous to the 2D $XY\pm$ vortex-point correlation $C(R) \sim R^{-\eta-(D-2)}$ as discussed in Sec. V.

---

*Present and permanent address.

[1](a) J. M. Kosterlitz and D. J. Thouless, J. Phys. C **6**, 1181 (1973); (b) V. Berezinskii, Zh. Eksp. Teor. Fiz. **61**, 1144 (1971) [Sov. Phys.—JETP **34**, 610 (1971)]; (c) A. P. Young, J. Phys. C **11**, L453 (1978).

[2]C. J. Lobb, Physica B+C **126B**, 319 (1984).

[3]J. Kosterlitz, J. Phys. C **7**, 1046 (1974).

[4]G. Kohring, R. Schrock, and P. Wills, Phys. Rev. Lett. **57**, 1358 (1986); G. Kohring and R. Schrock, Nucl. Phys. **B288**, 397 (1987).

[5]R. Feynman, in *Progress in Low Temperature Physics,* edited by C. Gorter (North-Holland, Amsterdam, 1955), Vol. I; Monte Carlo work monitoring the change in 3D XY loop geometry and size at transition has been done by W. Janke and H. Kleinert (W. Janke, Ph.D. thesis, Freie Universität, Berlin, 1985).

[6]J. Labastida, E. Sanchez-Velasco, R. Schrock, and P. Wills, Nucl. Phys. **B264**, 393 (1986).

[7]M. Lau and C. Dasgupta, Phys. Rev. B **39**, 7212 (1989).

[8](a) D. Nelson and J. Toner, Phys. Rev. B **24**, 363 (1981); (b) D. Nelson, in *Phase Transitions and Critical Phenomena,* edited by C. Domb and J. Lebowitz (Academic, New York, 1983), Vol. 7; (c) G. Grinstein, T. Lubensky, and J. Toner, Phys. Rev. B **33**, 3306 (1985).

[9](a) C. Dasgupta and B. Halperin, Phys. Rev. Lett. **47**, 1556 (1981); (b) J. Bartholomew, Phys. Rev. B **28**, 5378 (1983); Y. Munehisa, Phys. Rev. D **31**, 1522 (1985); (c) W. Janke and H. Kleinert, Phys. Rev. Lett. **57**, 279 (1980); J. Marchta and R. Cuyer, **60**, 2054 (1988).

[10](a) S. Chakravarty, S. Kivelson, G. Zimanyi, and B. Halperin, Phys. Rev. Lett. **35**, 7256 (1987); L. Jacobs, J. José, M. Novotny, and A. Goldman, Phys. Rev. B **38**, 4562 (1988); (b) V. Popov, Zh. Eksp. Teor. Fiz. **64**, 671 (1973) [Sov. Phys.—JETP **37**, 341 (1973)].

[11]H. M. Jaeger, B. de Havilland, A. Goldman, and B. Orr, Phys. Rev. B **34**, 4920 (1986).

[12]G. Baskaran and P. Anderson, Phys. Rev. B **37**, 580 (1988); A. Nakamura and T. Matsui, Phys. Rev. B **37**, 7940 (1988); D. Schmeltzer, Int. J. Mod. Phys. B **1**, 631 (1988); P. Anderson, S. John, G. Baskaran, B. Doucot, and S. Liang, Princeton report, 1988 (unpublished).

[13]J. Friedel, J. Phys. (Paris) **49**, 1561 (1988); **49**, 1769 (1988); D. Nelson, Phys. Rev. Lett. **60**, 1973 (1988); S. Martin, A. Fiory, R. Fleming, G. Espinosa, and A. Cooper, *ibid.* **62**, 677 (1989).

[14]D. Nelson and D. Fisher, Phys. Rev. B **16**, 4945 (1977).

[15]G. Williams, Phys. Rev. Lett. **59**, 1926 (1987); **61**, 1142(E) (1988).

[16](a) R. Savit, Phys. Rev. B **17**, 1340 (1978); Rev. Mod. Phys. **52**, 453 (1980); (b) J. Jose, L. Kadanoff, S. Kirkpatrick, and D. Nelson, Phys. Rev. B **16**, 1217 (1973).

[17](a) T. Banks, R. Myerson, and J. Kogut, Nucl. Phys. **B129**, 493 (1977); M. Einhorn and R. Savit, Phys. Rev. D **17**, 2583 (1980); (b) E. Fradkin, B. Huberman, and S. Shenker, Phys. Rev. B **18**, 4789 (1978).

[18]P. Weichmann, Phys. Rev. Lett. **61**, 2969 (1987); G. Kohring, R. Schrock, and P. Wills, *ibid.* **61**, 2970 (1987); B. Halperin, in *Physics of Defects,* Proceedings of the Les Houches Session No. XXXV (1980), edited by R. Balian, M. Kleman, and J.-P. Parier (North-Holland, New York, 1981).

[19]N. Gupte and S. Shenoy, Phys. Rev. B **31**, 3150 (1985).

[20]J. Gilliou and J. Zinn-Justin, Phys. Rev. B **21**, 3976 (1989), Tables III, V, and VI.

[21](a) A. Fetter, Phys. Rev. A **10**, 1724 (1974); (b) P. Roberts and J. Grant, J. Phys. A **4**, 55 (1971).

[22]P. Pfeuty and G. Toulouse, *Introduction to Renormalization Group and Critical Phenomena* (Wiley, New York, 1975), Sec. 5.3.

[23]S. Shenoy, J. Phys. C **18**, 5143 (1985); **18**, 5163 (1985); **20**, 2479(E) (1987).

[24]N. Gupte and S. Shenoy, Phys. Rev. D **33**, 3002 (1988); S. Shenoy and N. Gupte, Phys. Rev. B **38**, 2543 (1988).

[25]J. Jackson, *Classical Electrodynamics* (Wiley, New York, 1975), p. 181.

[26]We have not discussed the evaluation on symmetry breaking averages like $\langle \cos\theta_i \rangle$ or the nature of the ground state. In Ref. 24 we have attempted to describe the oriented-spin state in terms of oriented, average loops in a simple mean-field approach. The independently tumbling, nested, and growing loops considered in the scaling approach could be regarded as excitations destroying such order. An evaluation of topological loop moment correlations would be of interest.

[27]P. de Gennes, *Scaling Concepts in Polymer Chemistry* (Cornell University Press, Ithaca, 1979); I. Majid, Z. Djordjevic, and H. Stanley, Phys. Rev. Lett. **51**, 1282 (1983); S. Obhukov, J. Phys. A **17**, L965 (1984).

[28]The exponents depend on the solutions whose stability is investigated. One could linearize about the solutions $K_l^{-1} dK_l/dl = +1 = -y_l^{-1} dy_l/dl$, with $y_{l\_} = (A_0 K_{l\_})^{-1}$,

$\pi^2 K_{l_-} L_{l_-} = 7$ defining the dominant length. Then with a choice $\mu = \frac{1}{2} = -\theta$ in (3.14) the eigenvalues $\lambda_\pm = -1 \pm [1 + 7(1 - \theta/L_{l_-})]^{1/2}$ yield $\nu \simeq 0.548(1 - 0.34/L_{l_-})$. With a choice of constants $c_0 = 0.464$ and $K_{oc} = 0.348$ in $L_{l_-} = \frac{1}{2} l_- + \frac{1}{2} \ln K_{l_-} + (1 + c_0 - \frac{1}{2} \ln K_{oc}), \nu$ goes slowly to its $L_{l_-}^{-1} = 0$ value as $l_- \to \infty$. With $l_- = -0.5 \ln \epsilon_c$, and temperature cutoffs at $\epsilon_c = 10^{-5}$, 10^{-9}, and 0, one finds $\nu = 0.519$, 0.526, and 0.548. The solutions we consider, however, have $dK_l/dl|_{l=l_-}$ and $dy_l/dl|_{l=l_-} \to 0$ as $l_- \to \infty$, with fugacity falloffs as e^{-a} rather than e^{-l}.

[29]See, e.g., J. Choi and J. Josè, Phys. Rev. Lett. **62**, 320 (1988), and references therein; S. Shenoy, Phys. Rev. B **35**, 8652 (1987); Physica B+C **152B**, 72 (1988).

[30]T. Ohta and D. Jasnow, Phys. Rev. B **20**, 139 (1979).